BIOCHEMICAL PHARMACOLOGY 73 (2007) 1455–1462

available at www.sciencedirect.com

ScienceDirect

journal homepage: www.elsevier.com/locate/biochempharm

Pharmacokinetics of a hepatic stellate cell-targeted doxorubicin construct in bile duct-ligated rats

Rick Greupink [a], *Catharina Reker-Smit* [a], *Johannes H. Proost* [a], *Anne-miek van Loenen Weemaes* [a], *Marjolijn de Hooge* [b], *Klaas Poelstra* [a], *Leonie Beljaars* [a,*]

[a] *Department of Pharmacokinetics and Drug Delivery, University Centre for Pharmacy, Groningen University Institute for Drug Exploration (GUIDE), Antonius Deusinglaan 1, 9713 AV Groningen, The Netherlands*

[b] *Department of Nuclear Medicine, University Medical Centre Groningen, Hanzeplein 1, 9713 GZ Groningen, The Netherlands*

ARTICLE INFO

Article history:
Received 27 September 2006
Accepted 11 December 2006

Keywords:
Liver fibrosis
Drug targeting
Hepatic stellate cell
Selective delivery
Cytostatic drugs
Mannose-6-phosphate/insulin-like growth factor II receptor

ABSTRACT

Background/aims: Inhibition of hepatic stellate cell (HSC) proliferation is a relevant strategy to inhibit liver fibrosis. Coupling of antiproliferative drugs to the HSC-selective drug carrier mannose-6-phosphate-modified human serum albumin (M6PHSA) may lead to cell-selective inhibition of HSC proliferation. We coupled the antiproliferative drug doxorubicin (DOX) to this drug carrier and investigated the pharmacokinetics of this construct in a rat model of liver fibrosis, as well as in cultured HSC.

Methods/results: M6PHSA-DOX was cleared from the plasma in a biphasic manner. Upon i.v. injection of 4 $\mu g\,kg^{-1}$ (tracer), 2 and 20 $mg\,kg^{-1}$, the clearance in the distribution phase of drug disposition (CL_d) significantly decreased from 9.7 ± 0.7 to 4.7 ± 2.3 and $1.0 \pm 0.1\ ml\,kg^{-1}\,min^{-1}$, respectively. This indicates that saturation of clearance mechanisms occurs in this phase of drug disposition, likely reflecting saturable receptor-mediated uptake in the target cells. Gamma-camera studies revealed that the majority of the conjugate accumulated in the liver within 5 min, and immunohistochemical double-staining of liver sections demonstrated co-localization of the construct with HSC-markers. Simulation of the release of DOX from the carrier, after cellular uptake by HSC, showed that a gradual release of the drug takes place over a 9 h period. Studies in cultured HSC illustrated that after 24 h incubation with the conjugate, DOX was associated with the cell nucleus.

Conclusions: The rapid distribution of M6PHSA-DOX from the blood to HSC, in combination with the expected gradual release of DOX within these cells, make this construct a promising tool for achieving sustained and selective inhibition of HSC proliferation.

© 2006 Elsevier Inc. All rights reserved.

1. Introduction

Liver fibrosis is characterized by the excessive accumulation of collagen and other extracellular matrix proteins (ECM) as a result of chronic liver injury. The activated hepatic stellate cell (HSC) has been identified as the principal producer of these proteins in the fibrotic liver and therefore this cell type is considered a primary target for the development of new pharmacological treatments for this disease. Because HSC proliferation is a key event during fibrogenesis, the application of antiproliferative drugs for the treatment of this disease is a relevant option [1–3].

In previous work, we have identified doxorubicin (DOX) as a very potent inhibitor of HSC proliferation in vitro. Furthermore, we have shown that treatment of rats with experimental liver fibrosis with this antiproliferative drug significantly reduced the

* *Corresponding author*. Tel.: +31 503636414; fax: +31 503633247.
E-mail address: e.beljaars@rug.nl (L. Beljaars).

0006-2952/$ – see front matter © 2006 Elsevier Inc. All rights reserved.
doi:10.1016/j.bcp.2006.12.017

number of activated HSC in these diseased livers and also reduced collagen deposition [4]. However, serious adverse effects associated with the use of cytostatic drugs preclude their clinical use for the treatment of this chronic liver disease. Coupling of DOX to the HSC-selective drug carrier mannose-6-phosphate-modified human serum albumin (M6PHSA) may reduce the toxicity in non-target tissues.

M6PHSA has been designed to interact with mannose-6-phosphate/insulin-like growth factor-II receptors (M6P/IGF-II receptors) [5,6], which are upregulated on activated HSC [7–9]. After receptor binding, ligands are internalized and routed to the lysosomal compartment, in which the degradation of the receptor-bound proteins takes place [10]. By coupling drugs to M6PHSA, this route can be used for the selective delivery of drugs to M6P/IGF-II receptor bearing cells. Immunohistochemical studies that investigated the M6P/IGF-II receptor expression in experimental liver fibrosis secondary to bile duct ligation, revealed that the receptor is expressed on fibrogenic cells of the liver already during the early stages of experimental liver fibrosis [11].

Indeed, in vivo studies in rats with bile duct ligation (BDL)-induced liver fibrosis showed extensive co-localization of an M6PHSA-DOX conjugate with HSC markers [4]. However, information on the pharmacokinetics of this conjugate is still lacking. Such data are very important when employing HSC-targeted cytostatic drugs during liver disease. The experiments described in this paper therefore serve to gain a further understanding of the pharmacokinetics of M6PHSA-DOX in rats with experimental liver fibrosis. In addition, the paper investigates the release of DOX from its carrier by in vitro techniques, thus forming a basis for HSC-selective antiproliferative therapies aimed at reducing liver fibrosis.

2. Materials and methods

2.1. Experimental animals and experimental model of fibrosis

Male Wistar rats (Harlan, Horst, The Netherlands) of 220–240 g were housed under a 12 h dark/light cycle, at constant humidity and temperature. Animals had free access to tap water and standard lab chow (Harlan). All experiments were approved by the local committee for care and use of laboratory animals and were performed according to strict governmental and international guidelines for the use of experimental animals. Liver fibrosis was induced by ligation of the common bile duct (BDL) under O_2/N_2O/isoflurane anaesthesia as described previously [12].

2.2. Synthesis of M6PHSA-DOX

M6PHSA was synthesized and characterized as described by Beljaars et al. [6]. DOX (Pfizer, Capelle a/d IJssel, The Netherlands) was coupled to M6PHSA according to the method of Shen and Ryser as described previously [13]. Subsequently, M6PHSA-DOX was purified by extensive dialysis against PBS and size exclusion chromatography on a HiLoad Superdex column (GE healthcare, Den Bosch, The Netherlands) with PBS. After dialysis against water, the product was lyophilized and stored at −20 °C until use. The total amount of DOX and the amount of free DOX present in the preparation were quantitated by spectrophotometric analysis and HPLC analysis, respectively [4].

2.3. Radioactive labeling of HSA and M6PHSA-DOX

HSA and M6PHSA-DOX were labeled with ^{123}I for gamma-camera studies or with ^{125}I for plasma disappearance experiments, via a chloramine T method. Protein precipitation with trichloroacetic acid was performed to assess the percentage of free ^{123}I or ^{125}I in the preparations. To investigate whether the labeling procedure resulted in the formation of protein aggregates, we performed size exclusion chromatography on the constructs before administration to the animals. Radiochemical purity was determined by size exclusion HPLC. The system used consisted of a Waters 1500 series manual injector with a 20 μl injection loop (Rheodyne 7725i Injector, Milford, MA), a Waters 1525 binary HPLC pump, a Waters 2487 dual wavelength absorbance detector and an in-line radioactivity detector made of a sodium iodide crystal coupled to a multichannel analyzer. The size exclusion column used was a HR 16/300 Superdex 200 column (GE healthcare). Elution was performed with PBS at a flow of 1 ml min^{-1}.

2.4. Plasma disappearance

Ten days after BDL, when plasma bilirubin levels are high and hepatic fibrosis is evident [14], animals were anaesthetized as described above and the carotid artery was cannulated to allow rapid blood sampling. A single dose of 4 μg kg^{-1} (tracer, $n = 2$), 2 mg kg^{-1} ($n = 3$) or 20 mg kg^{-1} ($n = 3$) of M6PHSA-DOX was administered i.v. via the penis vein. To estimate the rate of plasma disappearance, unlabeled dosages of M6PHSA-DOX were supplemented with a tracer dose of 10^6 cpm of ^{125}I-labeled conjugate.

Blood samples were collected in heparinized tubes at 2, 5, 7, 10, 15, 30, 60, 90 and 120 min after administration, as described previously [15,16]. Blood samples were centrifuged at 7000 × g for 5 min to obtain plasma and subsequently, 100 μl of plasma was treated with an equal volume of 20% trichloroacetic acid to precipitate proteins. After centrifugation, the radioactivity in the pellet was counted with a γ-counter (Riastar, Packard instruments, Palo Alto, USA). Based on the amount of radioactivity in the pellet and the administered dosages of both radioactive as well as unlabeled material we calculated the total concentration of protein present in the plasma at the various time points after injection. Pharmacokinetic parameters were then derived from the data of individual animals, using the non-linear curvefitting program Multifit (Dr. J.H. Proost, Department of Pharmacokinetics and Drug Delivery, University of Groningen, The Netherlands).

2.5. Whole-body distribution and kinetics of hepatic uptake

Ten days after BDL, rats were anaesthetized with 0.4 ml kg^{-1} hypnorm in combination with 2 mg kg^{-1} diazepam intramuscularly. The rats were placed on the low-energy all-purpose

collimator of a gamma-camera and were i.v. injected with a tracer dose of ^{123}I-M6PHSA-DOX ($n = 3$). Additionally, three animals were injected with ^{123}I-HSA in order to be able to correct for blood-derived radioactivity. For analysis of the scans, the body area that encompasses the liver was highlighted in all rats, and the distribution of radioactivity to this area of interest was dynamically monitored from $t = 0$ to 20 min after injection with a frame-rate of one total body scan per 30 s. At the end of the 20 min scan-period, a final whole-body scan of 5 min was performed to assess the distribution at this time-point.

2.6. Intrahepatic distribution of M6PHSA-DOX

To investigate the intrahepatic distribution of the conjugate, fibrotic rats received a single i.v. injection of 2 or 20 mg kg^{-1} M6PHSA-DOX ($n = 3$ per group). Rats were sacrificed 20 min after injection and the livers were excised. On 4 μm cryostat sections of the livers immunohistochemical double-stainings were performed to determine the localization of the conjugate relative to markers for HSC [5]. As a marker for HSC, two monoclonal antibodies were combined: a mouse monoclonal IgG directed against desmin (Sigma) and mouse monoclonal IgG anti-GFAP (Neomarkers, Fremont, CA, USA), according to standard methods for HSC detection [17]. The conjugate itself was visualized with an antibody directed against HSA (Cappel, Zoetermeer, The Netherlands).

2.7. Drug release in buffer pH 4.5

To investigate whether DOX could be released from the conjugate in an acidic environment such as present in the lysosomal compartments of cells, M6PHSA-DOX was incubated for 0.75, 2, 3, 9, and 20 h in a 0.1 M Na_2HPO_4/citric acid buffer, pH 4.5. Release of DOX was monitored by injecting the samples onto an HPLC system fitted with a Waters pump (model 510), a μBondapack C18 guard column, a Thermoquest 250 mm × 4.6 mm 5 μm Hypersil BDS C8 column and a Waters UV detector (model 441) at 254 nm. A solution of 6.7 g trisodiumcitrate in 760 ml water and 240 ml acetonitrile (pH adjusted to 4 with formic acid) was used for elution at a flow of 1 ml min^{-1}. The amount of released DOX was then calculated from a calibration curve and related to the total amount of coupled DOX.

2.8. In vitro studies with HSC

Handling of the conjugate by HSC was assessed in vitro. HSC were isolated from male Wistar rats and cultured as described by Geerts et al. [18]. Seven days after isolation of HSC, 10,000 cells well^{-1} were plated onto glass LabTek incubation chambers (Nalge Nunc International, Rochester, NY, USA). Subsequently, after 2 days when HSC have a fully activated phenotype, HSC were incubated with 10 μg ml^{-1} of DOX or 50 μg ml^{-1} of M6PHSA-DOX for 2 and 24 h, at 37 °C. After washing, the doxorubicin-specific fluorescence in the cells was evaluated with a fluorescence microscope (Leitz, Wetzlar, Germany) equipped with a 450–490 nm excitation/>515 nm emission filter [19], without embedding the samples in mounting medium.

2.9. Statistical analysis

Results were expressed as the mean ± S.D. Data were subjected to a one-way analysis of variance followed by the LSD post hoc test and differences were considered statistically significant at $P < 0.05$. Statistical analyses were performed with the SPSS software package (SPSS Inc, Chicago, IL, USA).

3. Results

3.1. Synthesis of M6PHSA-DOX and radioactive labeling

The M6PHSA-DOX conjugate that was used for the present experiments contained 66.7 μg DOX per mg of the construct, reflecting a molar ratio of drug: protein of ~10:1, and only maximally 1% of total DOX was present in its unbound form. HSA, which was used to estimate blood-derived radioactivity in the gamma-camera study, and the DOX-containing conjugate were both successfully labeled without the formation of significant protein aggregates in the preparations (Fig. 1). Trichloroacetic acid (TCA) precipitation of the labeled constructs revealed that the HSA and M6PHSA-DOX preparations contained similar amounts of unbound iodine (between 5% and 10% free iodine), which allowed comparison of their body distribution via gamma-camera imaging. Size-exclusion chromatography was performed to investigate whether the labeling procedure resulted in the formation of large amounts of protein aggregates. In Fig. 1 it can be seen that the injected proteins contained only minor amounts of polymeric protein (monomeric peak at 30 min).

3.2. Plasma disappearance and pharmacokinetic parameters

In Fig. 2A–C, the plasma disappearance curves after i.v. injection of ^{123}I-labeled M6PHSA-DOX are displayed. To investigate how plasma-disappearance data could be best described, as a first estimation we fitted the parameters of one-, two- and three-compartment models to the plasma concentration data. The best fit, as assessed by calculation of Akaike's Information Criterion, was for all dosages obtained with a two-compartment model. The calculated pharmacokinetic parameters for a two-compartment model, assuming that elimination takes place from the peripheral compartment, are listed in Table 1. We found that initial half-life ($t_{1/2\alpha}$) significantly increased, and clearance in the distribution phase of disposition (CL_d) significantly decreased when the dose was increased to 20 mg kg^{-1} of M6PHSA-DOX. Clearance (CL), initial volume of distribution (V_1), apparent volume of the peripheral compartment (V_2), volume of distribution at steady state (V_{ss}) and terminal half-life ($t_{1/2\beta}$) did not significantly differ with the dose.

3.3. Whole-body distribution, kinetics of hepatic uptake and intrahepatic uptake

Gamma-camera studies were performed to assess the whole-body distribution of M6PHSA-DOX in time after i.v. injection (Fig. 3). Studies were performed 10 days after BDL when

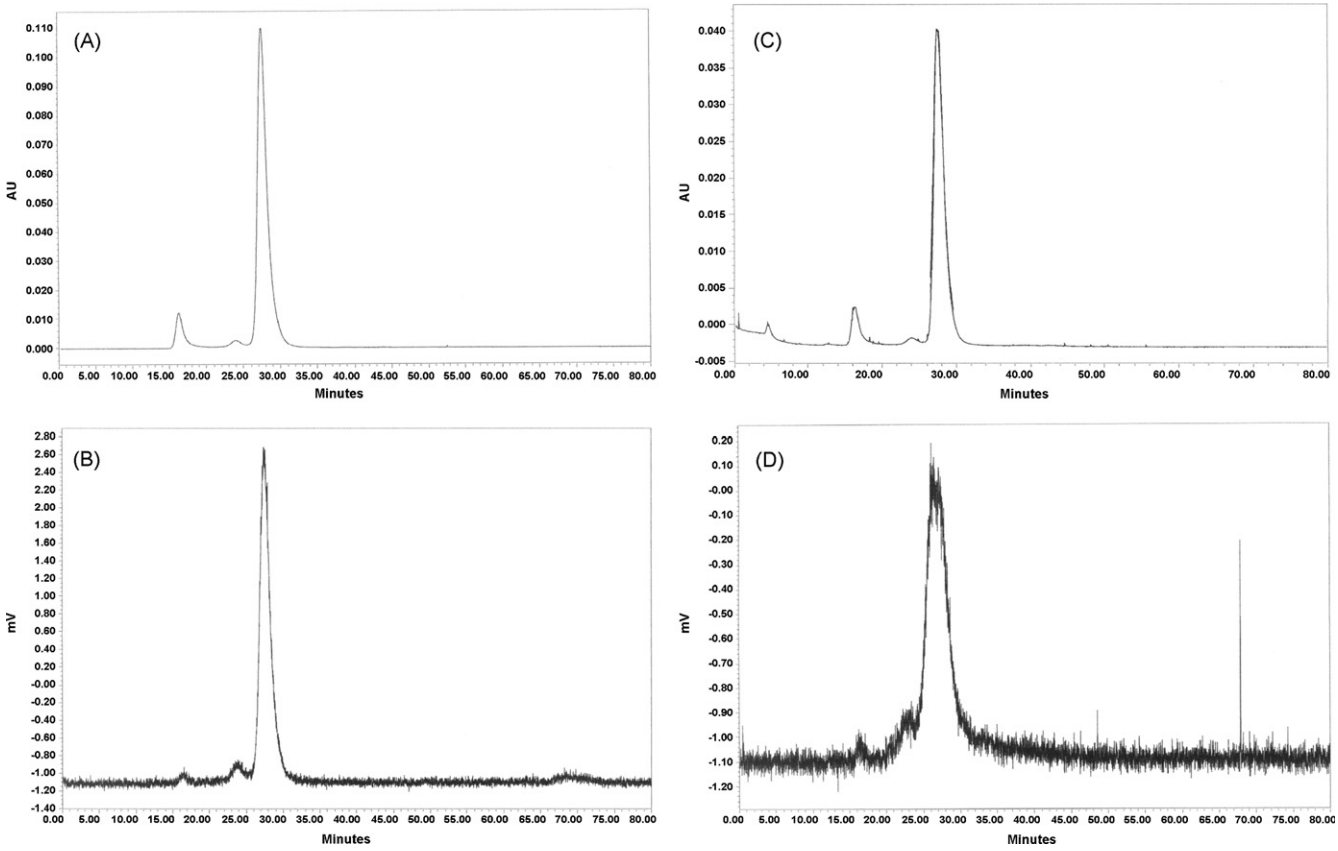

Fig. 1 – Size exclusion chromatograms of ^{123}I-labeled HSA (A and B) and ^{123}I-labeled M6PHSA-DOX (C and D). (A and C) On-line spectrophotometric detection of the proteins at UV_{280} nm. (B and D) Detection of the ^{123}I label in the same HPLC run. The retention time of the monomeric protein peak is 30 min.

fibrosis is rapidly progressing and HSC activation and proliferation is eminent [14]. First, ^{123}I-HSA was injected in order to estimate blood-derived radio-activity. After rapid distribution throughout the circulation within 30 s after injection, a constant blood-related background signal was found to be associated with well-perfused organs such as heart, lungs, kidneys and the liver (Fig. 3A and B). In contrast, after injection of M6PHSA-DOX, a rapid distribution to the livers was found, clearly exceeding those of HSA controls. Maximum levels in the livers were already reached within 5 min after injection. Signals in other organs were similar to those after injection of HSA (Fig. 3C and D).

Analysis of the intrahepatic distribution of the conjugate, 20 min after injection of 2 or 20 mg kg^{-1} indicated that the conjugate clearly co-localized with hepatic stellate cell markers (Fig. 3E), although some uptake could be observed in non-parenchymal cells that were not positive for HSC markers. In addition to this, we observed that after injection of a 2 mg kg^{-1} dose, this co-localization with HSC markers was confined to HSC in zones 2 and 3 of the liver, whereas after

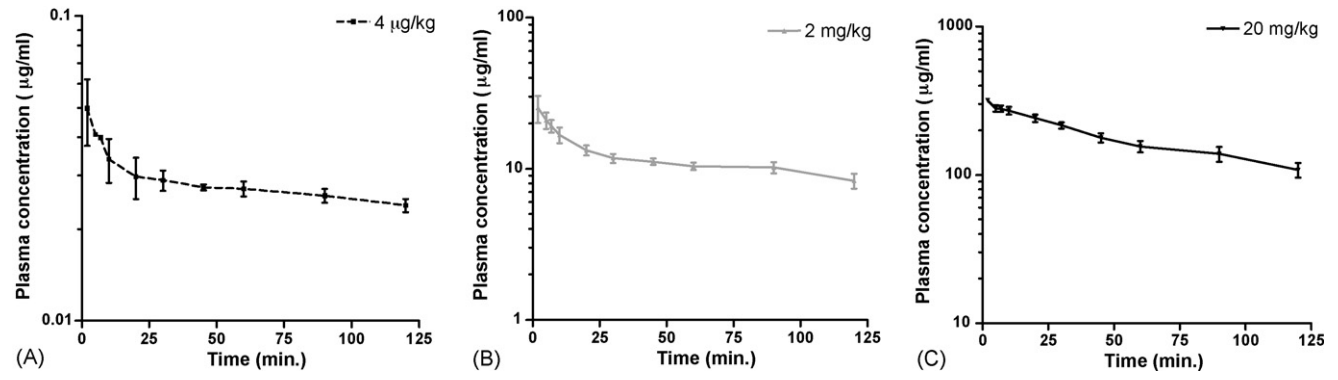

Fig. 2 – Plasma disappearance curves after injection of a 4 μg kg^{-1} tracer dose (A, $n = 2$), 2 mg kg^{-1} (B, $n = 3$) or 20 mg kg^{-1} (C, $n = 3$) M6PHSA-DOX in rats with liver fibrosis. Data are expressed as the mean ± S.D.

Table 1 – Pharmacokinetic parameters of M6PHSA-DOX administered i.v. to fibrotic rats

Parameter	4 μg kg^{-1} (n = 2)	2 mg kg^{-1} (n = 3)	20 mg kg^{-1} (n = 3)	Unit
$t_{1/2\alpha}$	2.29 ± 0.03	6.82 ± 3.86	26.0 ± 2.8*,†	min
$t_{1/2\beta}$	362 ± 180	246 ± 107	230 ± 50	min
CL_d	9.7 ± 0.7	4.7 ± 2.3	1.0 ± 0.1*,†	ml kg^{-1} min^{-1}
CL	0.28 ± 0.12	0.49 ± 0.18	0.38 ± 0.02	ml kg^{-1} min^{-1}
AUC_{0-120}	3.4 ± 0.4	1385 ± 194†	20790 ± 2515*,†	min μg ml^{-1}
V_t	67 ± 21	75 ± 33	64 ± 4	ml kg^{-1}
V_2	64 ± 9	85 ± 17	75 ± 31	ml kg^{-1}
V_{ss}	131 ± 11	160 ± 18	140 ± 32	ml kg^{-1}

Plasma concentration data of each animal were analysed separately using a two-compartment model with elimination from the peripheral compartment. Data are expressed as the mean ± S.D. †Indicates $P < 0.05$ compared to tracer-injected rats, *indicates $P < 0.05$ compared to rats injected with 2 mg kg^{-1} M6PHSA-DOX. $t_{1/2\alpha}$: initial half-life, $t_{1/2\beta}$: terminal half-life, AUC_{0-120}: area under the curve up to 120 min, CL_d: distribution clearance, CL: clearance, V_1: initial volume of distribution, V_2: apparent volume of the peripheral compartment, and V_{ss}: volume of distribution at steady state.

administration of the 20 mg kg^{-1} dose also distribution to the fibrotic portal areas (acinar zone 1) was observed (Fig. 3F).

3.4. *Drug release from the carrier*

To investigate the rate of drug release from the carrier in an acidic environment, M6PHSA-DOX was incubated in buffer pH 4.5. We found that drug release takes place over a period of approximately 9 h, amounting to a maximum release of approximately 30% of the total amount of coupled DOX, under the present test conditions (Fig. 4A). In vitro studies with rat HSC on the cellular handling M6PHSA-DOX revealed that after 24 h of exposure to the conjugate, DOX-specific fluorescence could be observed in the nucleus as well as in the cytoplasm of

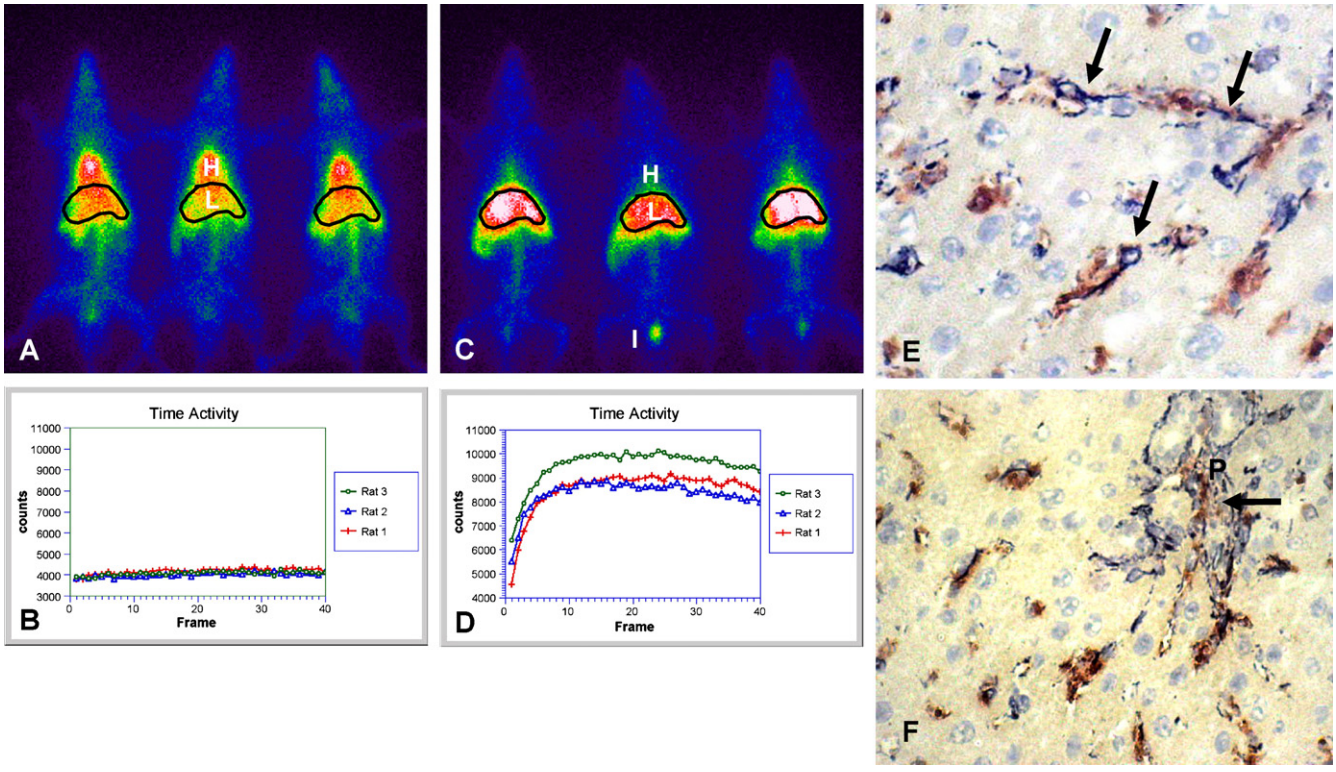

Fig. 3 – (A) Whole body scan taken with a gamma-camera at the end of the 20 min test period of three animals that received ^{123}I-labeled HSA. (B) Accumulation of ^{123}I-labeled HSA within the designated area of interest (the liver), as assessed by image analysis of consecutive γ-camera scans during the first 20 min after i.v. injection. (C) Whole body scan taken at the end of the 20 min test period of three animals that received ^{123}I-labeled M6PHSA-DOX. D: Association of radio-activity with the liver region during the first 20 min after i.v. injection of ^{123}I-labeled M6PHSA-DOX. (E) Double-staining for M6PHSA-DOX (red staining) with HSC markers (blue staining) in liver sections. (F) After injection of the 20 mg kg^{-1} dose, also double-positive cells were found in the more fibrotic portal areas of the liver. P marks a portal area (acinar zone 1). Arrows indicate co-localization of the construct with HSC markers, original magnification 200×. In the whole body scans, H indicates heart, L indicates liver, and I indicates the injection site.

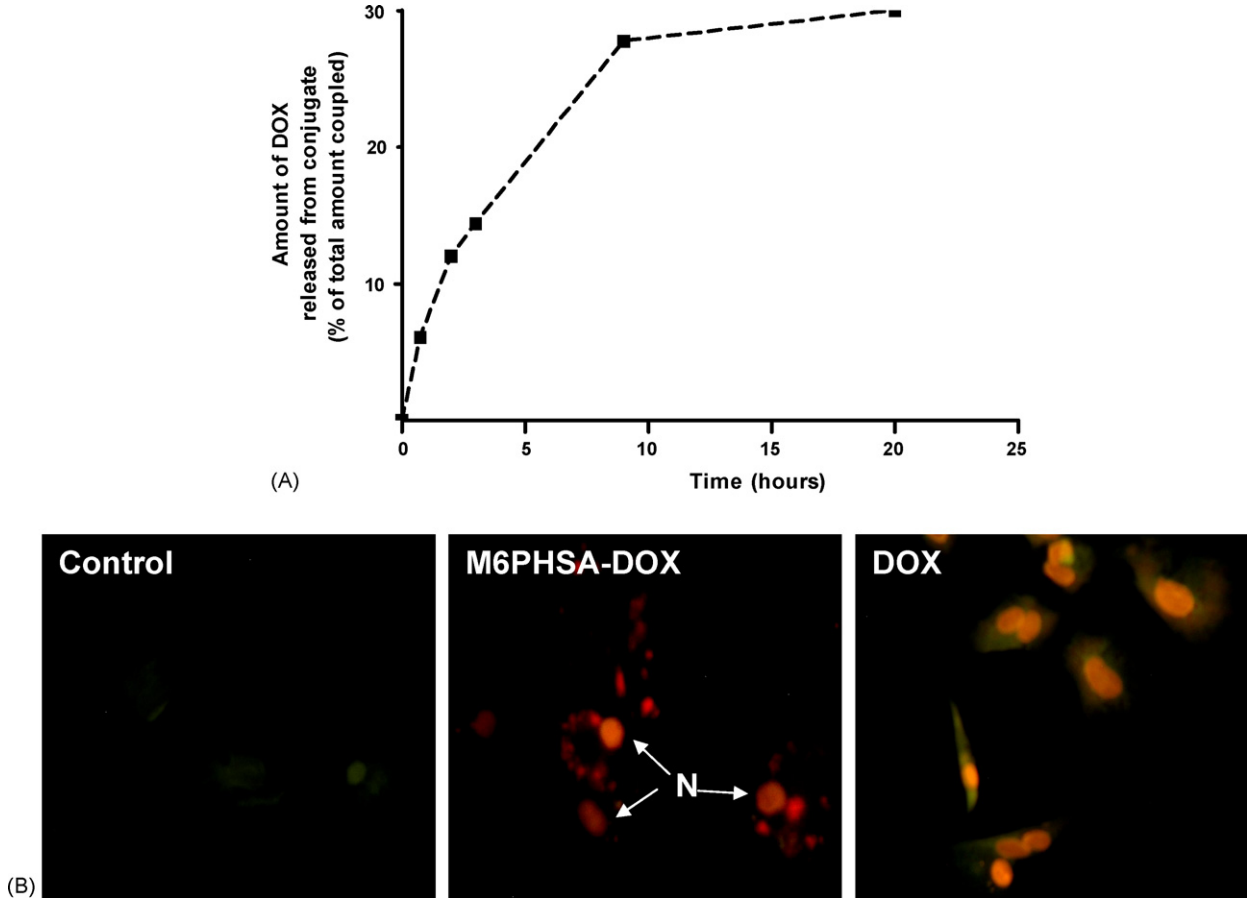

Fig. 4 – (A) Typical example of an experiment investigating the release of DOX from the conjugate in buffer pH 4.5. (B) Fluorescence microscopy study of the binding and uptake of M6PHSA-DOX in activated rat HSC. The red fluorescent pattern (excitation wavelength 450–490 nm emission wavelength >515 nm) reflects DOX itself. Uncoupled DOX accumulates only in the nuclei of HSC, whereas in the M6PHSA-DOX-treated cells, DOX-specific fluorescence is located in the cytoplasm as well as in the nuclei. Arrows in B indicate the nuclei in M6PHSA-DOX-treated cells. The micrographs are representative for data obtained with HSC from three different isolations (original magnification 200×).

HSC (Fig. 4B). It is likely that the cytoplasmic localization reflects the presence of the conjugate in the lysosomal compartment of the cell after receptor-mediated uptake. The observed association of fluorescence with the nucleus suggests that DOX is also being released from its carrier upon incubation with HSC and is able to translocate to the cell nucleus. In contrast, cells incubated with unconjugated DOX only showed association of fluorescence with nuclei, and no cytoplasmic staining pattern was found (Fig. 4B). In contrast to the M6PHSA-DOX-treated cells, the DOX-specific nuclear fluorescence in cultures that were incubated with uncoupled DOX could already be observed after 2 h of incubation, which is in line with the known capability of uncoupled DOX to diffuse freely and rapidly across membranes.

4. Discussion

Inhibition of HSC proliferation poses a relevant strategy to inhibit liver fibrosis. However, selective delivery of antiproliferative drugs will be essential to avoid systemic side effects and allow these drugs to be used in a clinical setting for treatment of chronic liver diseases [1,3]. Although tumour-specific delivery of cytostatics is a well-established strategy, the targeted delivery of antiproliferative drugs to the principal fibrogenic cell type in the liver is a new field of research. This study describes the pharmacokinetic profile of an HSC-targeted construct containing doxorubicin. We found that M6PHSA-DOX is cleared in a biphasic pattern from the circulation, distributes to the liver within minutes and accumulates in the cytoplasm and nuclei of HSC. Moreover, the present in vitro studies revealed that after this rapid initial distribution of the conjugate to the target cells, a gradual release of the drug can be expected within HSC.

From earlier studies it is known that M6P-modified proteins are internalized by HSC via receptor-mediated endocytosis. In these previous in vitro studies we showed that binding and uptake of M6PHSA conjugates occurs within the isolated target cells, and that this process is saturable [5,6,20]. In the present in vivo experiments we found that the clearance in the initial phase of the curves decreased upon an increase in dose from 2 to 20 mg kg^{-1}. In view of our knowledge on receptor-mediated

endocytosis of M6PHSA-conjugates in vitro, this observation likely reflects that saturation of receptor-mediated hepatic uptake is taking place in the given dosage range. Based on these current insights, it would be more appropriate to analyze the dose-dependent plasma disappearance pattern according to a model including a Michaelis–Menten type of kinetics in the initial phase of the curve, describing the receptor-mediated transfer from the plasma compartment to the second compartment (liver). Using a population-based approach, as described earlier [21], which includes such a Michaelis–Menten transport process from the central to the peripheral compartment, in the two-compartment pharmacokinetic model with elimination from the peripheral compartment, a V_{max} of 400 $\mu g\,min^{-1}\,kg^{-1}$ and K_m of 50 $\mu g\,ml^{-1}$ could be roughly estimated. Since V_1 is approximately 70 $ml\,kg^{-1}$ in the studied population, this implies that at dosages exceeding 3.5 $mg\,kg^{-1}$, initial plasma decay and hepatic uptake will be significantly slower than at linear conditions ($C_{pl} \ll K_m$). However, studies that investigate the pharmacokinetics of M6PHSA-DOX in BDL rats across a wider dosage range will be needed to determine these parameters more accurately. Nevertheless, our observations imply that in multiple dosing schemes, at relatively high dosages, the dosing frequency of M6PHSA-DOX may be reduced, which can be considered favourable for the administration of drugs via the intravenous route.

Data from the γ-camera studies indicated that the vast majority of injected construct accumulated in the liver. This is in line with results from an earlier study in which the organ distribution of M6PHSA-DOX was studied in rats with liver fibrosis only at one fixed time-point, 20 min after injection, by excision of organs and measuring the radioactivity that accumulated within the various organs [4]. The main novelty of the present study therefore is that it also describes the time-course of this hepatic uptake, which revealed that major hepatic uptake already takes place within the first minutes after injection and plateau levels are reached within 5 min.

It should be realized however that many modified proteins are taken-up by the liver, by virtue of scavenger receptor-mediated clearance by the mononuclear phagocyte system [22,23]. Indeed, as also the case for tumour-targeted proteins, intrahepatic uptake of M6PHSA-DOX by macrophages and endothelial cells was observed. However, a clear co-localization of the HSC-targeted DOX construct with HSC-markers was found in our studies, indicative of substantial uptake by these target cells during active liver disease.

Although techniques to study the disposition of HSC-targeted constructs at the body and organ level are readily available, investigation of drug disposition after release from the carrier within HSC in vivo is still technically cumbersome. We therefore studied the release of DOX from the conjugate in vitro and found that drug release from the carrier occurs relatively slow. Besides DOX-specific fluorescence within granular structures in the cytoplasm, 24 h incubation of cells with M6PHSA-DOX, also resulted in association of the cytostatic drug with the nuclei of the cells. The observed cytoplasmic accumulation likely reflects the uptake op M6PHSA-DOX into lysosomes, since it has been shown that ligands of M6P/IGF-IIR are routed to this cellular compartment after internalization [6,10]. Because a direct translocation of intact albumin-based constructs to the nucleus is very unlikely after lysosomal uptake, the data indicate that degradation of the construct and subsequent drug release takes place in these cells. The fact that immunohistochemical staining of cells incubated with M6PHSA-conjugates for HSA in revealed the nuclei to be negative for the intact conjugate, strengthens this notion [5,6]. Moreover, previous studies from our lab [4] showed that M6PHSA-DOX successfully inhibited HSC proliferation in vitro, also indicating that pharmacologically active DOX is set free from the carrier within these cells. Yet, drug release in acidic buffer was not complete. This may be explained by the fact that upon conjugation of DOX to the drug carrier an acid-stable stereo-isomer between DOX and the *cis*-aconityl linker is formed besides the formation of the desired acid-sensitive stereo-isomer [13]. In future studies, the percentage of DOX that is released from the conjugate should therefore be optimized by the insertion of different linkers between the drug and the carrier. However, it is very well possible that in vivo proteases degrade the carrier and additionally contribute to the release of DOX.

The slow rate of drug release may prove an advantage since this may result in a sustained antiproliferative effect within cells even after a single i.v. injection. However, intracellular levels will also depend on the rate of elimination of DOX from HSC. One major elimination pathway for this type of drugs from cells in general, is via active transport by membrane proteins belonging to the ATP binding cassette (ABC) transporter family. In the rat, DOX efflux from cells is mainly mediated by the drug transporters mdr1a and mdr1b, the rodent homologues of human *P*-glycoprotein (Pgp) [24]. Interestingly, Hannivoort et al. demonstrated the presence of mRNA transcripts encoding mdr1a and mdr1b in cultures of activated HSC [25]. Yet, to our knowledge there are no studies that have investigated whether the presence of these mRNAs also translates into the presence of a functional drug efflux system in HSC. However, the possible presence of relevant drug efflux pumps with respect to DOX, emphasizes the need for more detailed studies concerning the mechanisms of drug elimination by this particular cell type.

In conclusion, the rapid distribution of M6PHSA-DOX from the blood to the liver in combination with the sustained release of DOX that is expected to take place in the target cells, make this construct a promising tool for achieving a selective inhibition of HSC proliferation during liver fibrosis. Since proliferation of HSC is a key event during fibrogenesis, attenuation of this process may be highly relevant. Currently, studies on the efficacy of this drug delivery construct in experimental liver fibrosis are in progress.

Acknowledgements

The help of Mr. J.H. Pol and Mr. H. ter Veen during these studies is greatly appreciated. Mrs. H.I. Bakker and pharmacy students W. Bouma and M. de Ruijter are thanked for their assistance during in vitro experiments. Mrs. A. de Jager-Krikken and Prof. D.K.F. Meijer are gratefully acknowledged for performing immunohistochemical double-stainings and critical review of the manuscript, respectively. This work was financially supported by the Dutch Foundation for Technical Sciences.

REFERENCES

[1] Pinzani M, Rombouts K, Colagrande S. Fibrosis in chronic liver diseases: diagnosis and management. J Hepatol 2005;42 Suppl:S22–36.
[2] Bataller R, Brenner DA. Hepatic stellate cells as a target for the treatment of liver fibrosis. Semin Liver Dis 2001;21:437–51.
[3] Bataller R, Brenner DA. Liver fibrosis. J Clin Invest 2005;115:209–18.
[4] Greupink R, Bakker HI, Bouma W, Reker-Smit C, Meijer DK, Beljaars L, et al. The antiproliferative drug doxorubicin inhibits liver fibrosis in bile duct-ligated rats and can be selectively delivered to hepatic stellate cells in vivo. J Pharmacol Exp Ther 2006;317:514–21.
[5] Beljaars L, Molema G, Weert B, Bonnema H, Olinga P, Groothuis GM, et al. Albumin modified with mannose 6-phosphate: a potential carrier for selective delivery of antifibrotic drugs to rat and human hepatic stellate cells. Hepatology 1999;29:1486–93.
[6] Beljaars L, Olinga P, Molema G, de Bleser P, Geerts A, Groothuis GM, et al. Characteristics of the hepatic stellate cell-selective carrier mannose 6-phosphate modified albumin (M6P(28)-HSA). Liver 2001;21:320–8.
[7] de Bleser PJ, Jannes P, van Buul-Offers SC, Hoogerbrugge CM, van Schravendijk CF, Niki T, et al. Insulinlike growth factor-II/mannose 6-phosphate receptor is expressed on CCl4-exposed rat fat-storing cells and facilitates activation of latent transforming growth factor-beta in cocultures with sinusoidal endothelial cells. Hepatology 1995;21:1429–37.
[8] Weiner JA, Chen A, Davis BH. E-box-binding repressor is down-regulated in hepatic stellate cells during up-regulation of mannose 6-phosphate/insulin-like growth factor-II receptor expression in early hepatic fibrogenesis. J Biol Chem 1998;273:15913–9.
[9] de Bleser PJ, Scott CD, Niki T, Xu G, Wisse E, Geerts A. Insulin-like growth factor II/mannose 6-phosphate-receptor expression in liver and serum during acute CCl4 intoxication in the rat. Hepatology 1996;23:1530–7.
[10] Dahms NM, Hancock MK. P-type lectins. Biochim Biophys Acta 2002;1572:317–40.
[11] Greupink R, Bakker HI, van Goor H, de Borst MH, Beljaars L, Poelstra K. Mannose-6-phosphate/insulin-Like growth factor-II receptors may represent a target for the selective delivery of mycophenolic acid to fibrogenic cells. Pharm Res 2006;23:1827–34.
[12] Beljaars L, Poelstra K, Molema G, Meijer DK. Targeting of sugar- and charge-modified albumins to fibrotic rat livers: the accessibility of hepatic cells after chronic bile duct ligation. J Hepatol 1998;29:579–88.
[13] Shen WC, Ryser HJ. *cis*-Aconityl spacer between daunomycin and macromolecular carriers: a model of pH-sensitive linkage releasing drug from a lysosomotropic conjugate. Biochem Biophys Res Commun 1981;102:1048–54.
[14] Hines JE, Johnson SJ, Burt AD. In vivo responses of macrophages and perisinusoidal cells to cholestatic liver injury. Am J Pathol 1993;142:511–8.
[15] Swart PJ, Beljaars L, Kuipers ME, Smit C, Nieuwenhuis P, Meijer DK. Homing of negatively charged albumins to the lymphatic system: general implications for drug targeting to peripheral tissues and viral reservoirs. Biochem Pharmacol 1999;58:1425–35.
[16] Swart PJ, Hirano T, Kuipers ME, Ito Y, Smit C, Hashida M, et al. Targeting of superoxide dismutase to the liver results in anti-inflammatory effects in rats with fibrotic livers. J Hepatol 1999;31:1034–43.
[17] Geerts A. History, heterogeneity, developmental biology, and functions of quiescent hepatic stellate cells. Semin Liver Dis 2001;21:311–35.
[18] Geerts A, Niki T, Hellemans K, De Craemer D, Van Den Berg K, Lazou JM, et al. Purification of rat hepatic stellate cells by side scatter-activated cell sorting. Hepatology 1998;27:590–8.
[19] Ismail AA, Amin AM. Cytofluorescence evidence of adriamycin in liver. Neoplasma 1982;29:735–40.
[20] Greupink R, Bakker HI, Reker-Smit C, Loenen-Weemaes AM, Kok RJ, Meijer DK, et al. Studies on the targeted delivery of the antifibrogenic compound mycophenolic acid to the hepatic stellate cell. J Hepatol 2005;43:884–92.
[21] Proost JH, Beljaars L, Olinga P, Swart PJ, Kuipers ME, Reker-Smit C, et al. Prediction of the pharmacokinetics of succinylated human serum albumin in man from in vivo disposition data in animals and in vitro liver slice incubations. Eur J Pharm Sci 2006;27:123–32.
[22] Terpstra V, van Amersfoort ES, van Velzen AG, Kuiper J, van Berkel TJ. Hepatic and extrahepatic scavenger receptors: function in relation to disease. Arterioscler Thromb Vasc Biol 2000;20:1860–72.
[23] Jansen RW, Molema G, Harms G, Kruijt JK, van Berkel TJ, Hardonk MJ, et al. Formaldehyde treated albumin contains monomeric and polymeric forms that are differently cleared by endothelial and Kupffer cells of the liver: evidence for scavenger receptor heterogeneity. Biochem Biophys Res Commun 1991;180:23–32.
[24] Leslie EM, Deeley RG, Cole SP. Multidrug resistance proteins: role of P-glycoprotein, MRP1, MRP2, and BCRP (ABCG2) in tissue defense. Toxicol Appl Pharmacol 2005;204:216–37.
[25] Hannivoort RA, Buist-Homan M, Faber KN, Moshage H. MRP-type transporters protect activated hepatic stellate cells against cell death. Hepatology 2004;40:615A.